Journal of
Ship&Ocean
Technology

SOTECH Vol.1, No.1; pp.1~14

Effect of Structural Elasticity on Slamming Against Wetdecks of Multihull Vessels

Jan Kvålsvold[1], Odd M. Faltinsen[2], Jan V. Aarsnes[3]

[1] Det Norske Veritas Classfication AS, Høvik, Norway
[2] The Norwegian Institute of Technology, Trondheim, Norway
[3] MARINTEK, Trondheim, Norway

Abstract

Hydroelastic slamming against the wetdeck of a multihull vessel is studied numerically and experimentally. The beam equations and a two-dimensional flow model are used to find the dynamic stresses in longitudinal stiffeners between two transverse stiffeners. The largest stresses in the structure occur in the time scale of the lowest wet natural period of the beam. A simple relation between the maximum stress, the local geometry and the impact velocity of the wetdeck is established. The stresses in the wetdeck are neither sensitive to the radius of curvature of the waves nor where the waves initially hit the wetdeck. It is concluded that the maximum impact pressure should not be used to find maximum bending stresses during wetdeck slamming.

1. Introduction

Impact between the water and a ship, i.e. slamming, can cause important local and global loads on a vessel. Slamming is often categorized as bottom slamming, bow flare slamming and wetdeck slamming. By wetdeck is meant the structural part connecting the two side hulls of a catamaran. The present study shows that hydroelastic effects are important for the local behaviour of the wetdeck during a slam event. By hydroelastic effects are meant that the hydrodynamic loads are a function of the structural deformations. A slamming model where the local hydroelastic effects are accounted for, is not so frequently appearing in the literature. However, Meyerhoff [1965] studied slamming against elastic two-dimensional wedges penetrating an initially calm free water surface. Kvålsvold and Faltinsen [1944,1995] studied the hydroelastic effects during impact between a free water surface and an elastic wetdeck of a multihull vessel. In this paper the numerical method by Kvålsvold and Faltinsen [1994] is extended and compared with the drop tests by Aarsnes [1994]. The hydrodynmic loads in the theoretical method account for the vibrations of the structure and are based on an extension of Wagner's [1932] two-dimensional asymptotic theory. In order to have a numerically stable time integration procedure, it was found necessary to express the loads by an extensive use of analytical functions. The interaction effects between the local hydroelastic response of the wetdeck is scaled by separating the water impact into three phases. Each phase has its own time scale. The three impact phases are called the compressibility phase, the structural inertia phase and the added mass-restoring phase. When the impact velocity is not too small, it is found numerically and experimentally that the local bending

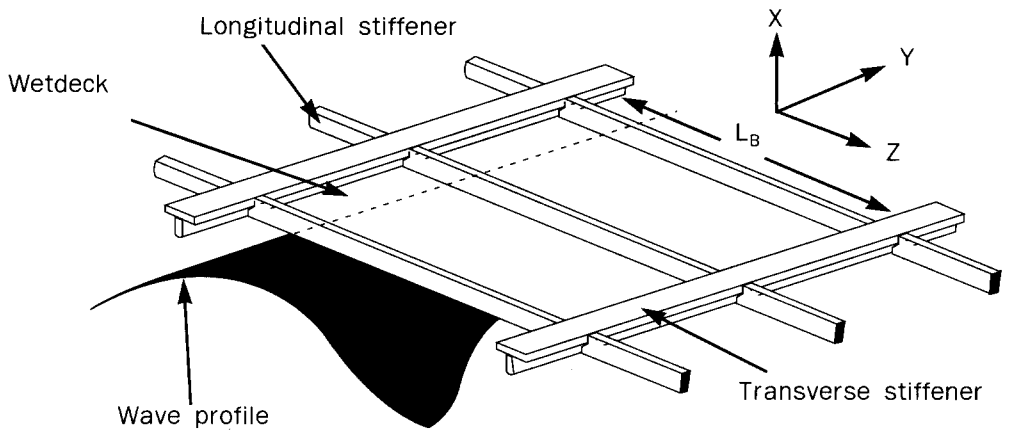

Figure 1. A detail of the wetdeck structure of a multihull vessel

stresses in the wetdeck are not sensitive to the local details of the wave shape and where the waves initially hit.

2. Theoretical Background

A detail of the wetdeck structure of a multihull vessel is shown in Figure1. The right-handed *xyz*-coordinate system is a local coordinate system that moves with the forward speed U of the vessel. The x-axis is parallel to the longitudinal stiffeners and is pointing towards the stern of the vessel. The origin of the local coordinate system is located midways between two of the transverse stiffeners in the wetdeck. The part of the wetdeck between two of the transverse stiffeners is modelled as a Timoshenko beam with length L_B corresponding to the distance between the transverse stiffeners. This means that the beam deflections are dominated by those of the longitudinal stiffeners. Local deformations of the plate field between two of the longitudinal stiffeners cause a three-dimensional hydrodynamic effect that is not covered by this analysis. The transverse stiffeners are assumed to be much stiffeners can be disregarded. Rotatory springs are introduced at the beam ends to account for the restoring moment of the part of the wetdeck structure outside the modelled beam. k_θ is the spring stiffness that is related to the restoring moment $M_r = -k_\theta \theta_{be}$ where θ_{be} is the rotation angle at the beam end. No axial force effects are considered. The curvature of the wetdeck in the water impact region is not accounted for in the structural formulation. It is assumed that the crest of a regular wave system hits the wetdeck midways between two of the transverse stiffeners in the wetdeck. Furthermore, it is assumed that the wetdeck is horizontal in the impact region, so that both the beam deflections as well as the local fluid flow are symmetric about a vertical plane through the line of the initial water impact.

The Timoshenko beam equations of motions are used as a basis for the numerical model of the hydroelastic response. The hydrodynamic impact pressure $p(x, w, t)$ is used as an external force per unit area of the Timoshenko beam. t is the time variable. $w(x, t)$ is the elastic beam deformation interpreted as the difference between the actual vertical position of the wetdeck and

the vertical position due to the global rigid heave and pitch motions of the vessel. The beam deflections are expressed in terms of the beam's dry normal modes in this work.

In order to find the hydrodynamic pressure p, one needs to solve a hydrodynamic boundry value problem. A simplified symmetric hydrodynamic boundary value problem is defined, based on a generalization of Wagner's [1932] asymptotic theory. The theory is valid for small local angles between the undisturbed water surface and the body surface in the impact area. acceleration of gravity, air pocket effects, cavitation and ventilation are neglected. It should be noted that this approach implies infinite pressure at the ends of the wetted length when $dc(t)/dt$ is not equal zero. Here $2c(t)$ is the wetted length of the beam. For further details of the theoretical formulation and the solution procedures, references are made to Kvålsvold and Faltinsen [1994,1995].

The slamming problem can be divided into three time phases. The first phase is called the compressibility phase. In this impact phase $dc(t)/dt > C_e$ where C_e is the speed of sound in water. $dc(t)/dt$ is the velocity of the geometric intersection line between the undisturbed water surface and the wetdeck The time scale of this impact phase is associated with the time it takes until $dc(t)/dt=c_e$, i.e. $|V|R/c_e^2$. R is the radius of curvature of the waves at the line of the initial water impact. For incident waves of small amplitudes $|V|$ R is expressed as, $(k^2\zeta_a)^{-1}$where k is the wave number. The second impact phase is called the structural inertia phase. The total hydrodynamic force is balanced by the structural inertia forces of the beam element in this impact phase. This causes very large accelerations of the beam, so that the mean value, in space over the wetted length, of the vertical vibration velocity is almost equal to the drop speed L_B^2 at the end of the structural inertia phase. The time scale of the structural inertia phase is associated wit the time it takes until the beam is totally wet, i.e. $L_B^2/(R|V|)$. The third impact phase is denoted the added mass-restoring phase. The beam is then totally wet. The inertia forces due to the added mass of the beam are much larger than the inertia forces associated with the structural mass in the third impact phase. The restoring forces due to bending of a beam element and the added mass inertia force of the beam balance each other approximately and determine the time scale T. It follows that $T = (\rho L_B^5/EI)^{1/2}$. This is approximately proportional to the first wet natural period of the beam. ρ is the mass density of water. EI is the bending stiffness, so that E is the Youngs modules and I is the area moment of inertia of the beam cross section. The maximum response in terms of local bending stresses in the wetdeck occurs in this impact phase. Thus, the time scale of the third impact phase is used as the time scale of the local hydroelastic slamming problem. The hydrodynamic forces not associated with the added mass forces are small and dependent on the relative velocities between $|V|$ and $\partial w(x,t)/\partial t$. We therefore make $\partial w(x,t)/\partial t$. non-dimensional by $|V|$. Subsequently, by using the time scale, the beam deformation scale becomes $|V|(\rho L_B^5/EI)^{1/2}$ In order for the presented scaling to be the proper scaling of the hydroelastic response, the third time phase has to be much larger than the two first phases. The fraction between the third and the second time scale is proportional to $|V|R$. This implies that the product of the drop speed and the radius of curvature of the wave crests should not be too small in order for this scaling to be the proper scaling of the hydroelastic response. Non-dimensional groups of parameters can be constructed by making the governing beam equations of motions non-dimensional using the scales for time, length, velocity and deflection [Kvålsvold and Faltinsen 1995].

It should be noted that the acceleration of gravity is not included in the non-dimensional coefficient. However, the gravity is implicitly included in $|V|$, since $|V|$ mainly comes from the global rigid ship motions that are Froude scaled. A proper scale for the bending stress scale is

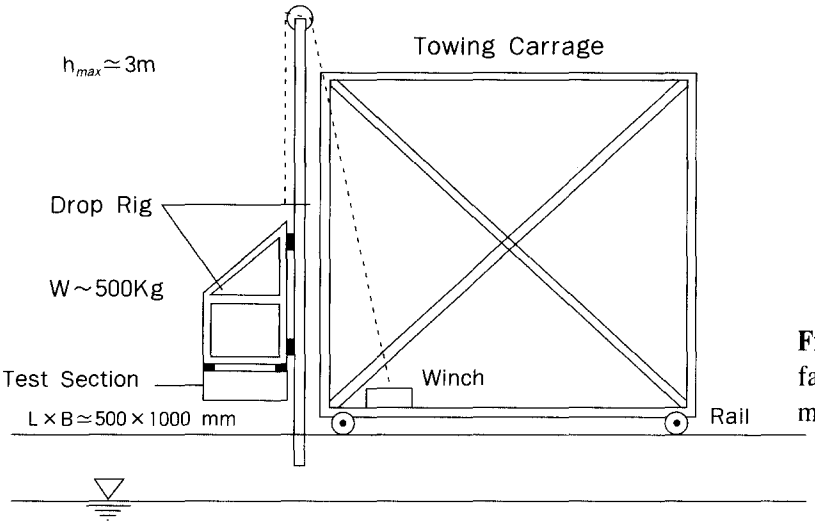

Figure 2. A sketch of the free-falling rig. h_{max} is the maximum drop height

found to be $T = (\rho L_B^5 E / I)^{1/2}$. The expression of the bending stress introduces the non-dimensional parameter z_{na} / L_B. z_{na} is the distance from the neutral axis in the beam cross section area to the monitoring point for the stresses. The effect of shear stresses is found to be small.

Faltinsen (unpublished) has shown analytically and numerically that if the two first time scales are small relative to the third time scale, the results in the third time scale can be found by solving an approximate initial value problem for the wetted beam. This highly simplifies the hydroelastic problem. The initial conditions are zero deflection and a spatially constant deflection velocity equal to the drop speed $|V|$. A few wet modes are needed in the analysis. This will also apply for a three-dimensional analysis. The third time scale is obviously very small relative to the global natural periods for the whipping response. A consequence is that local hydroelastic effects will die out during the time scale of the whipping response. It is therefore anticipated that the wetdeck can be considered locally rigid in a whipping analysis.

3. Test Arrangements and Test Program

To perform the drop tests a new free-falling rig has been developed. The rig consists of three different parts; the test sections, the trolley to which the test sections are connected and the vertical guide rails. A sketch of the free-falling rig is shown in Figure 2. The test sections are mounted directly to the trolley, which is engaged with the vertical guide rails. The total horizontal dimensions of the test sections are L x B = 1.0 m x 0.5 m. The free-falling rig is connected to the front of the towing carriage as shown in Figure 2. The test sections are connected to the trolley during the entire drop. In this way any rotation of the test sections are suppressed even during the impact phase. The trolley is raised using a winch fitted with a quick-release hook. After the test section has hit the water surface, the trolley is stopped using two elastic ropes. The hook is connected to an automatic release mechanism which is coupled to a wave gauge. The rig is released at a prescribed wave elevation. In this way the drop position relative to the wave crest can be selected by moving the wave gauge. In addition, a wave gauge was located at the side of the drop section to check the wave elevation during the impact.

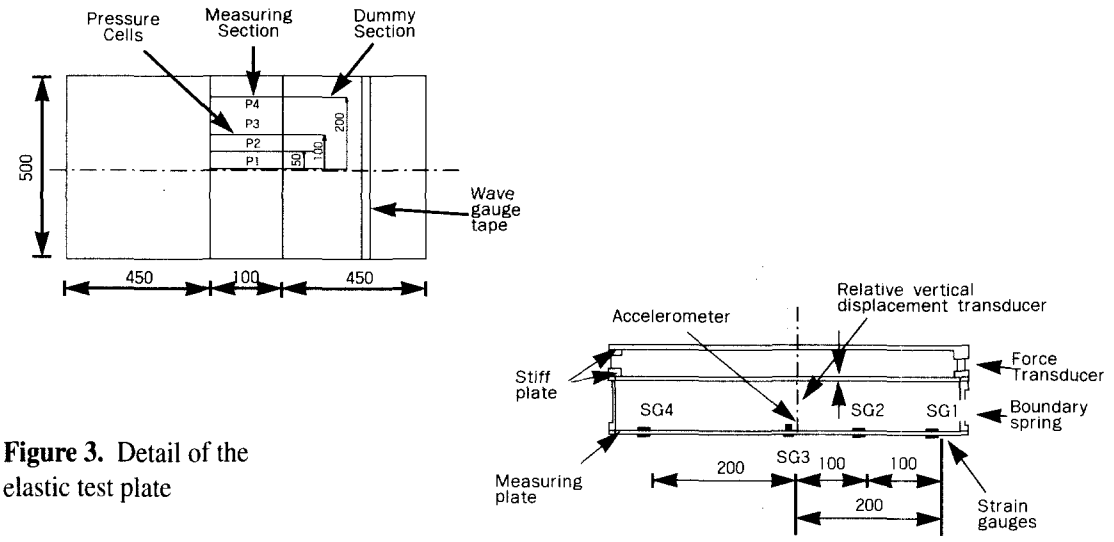

Figure 3. Detail of the elastic test plate

During the tests both a stiff and an elastic horizontal plate were tested. The shape of the different plates are shown in Figure 3. However, only the elastic plate is considered in this paper. The plate is intended to represent the wetdeck structure between two transverse stiffeners, similar to the beam in the theoretical model. In this study, steel is selected as the basis for the wetdeck material. The total drop section was divided into three parts, one measuring section with a dummy section on each side as shown in the figure. The measuring section was connected to the rig using two force transducers. The total weight of the measuring section includes the weight of the test plate in addition to the support system of the plate, i.e. it represents the total weight of the section connected underneath the vertical force transducers (see Figure 3). This weight is $14kg$. The thickness of the elastic plate was 8 *mm*. The material density is 7850 kg/m^3 and the E modulus is 210×10^9 N/m^2. The thickness and the stiffness of the dummy section plates were the same as for the measuring section. The total weight of the drop rig was 500 kg.

The instrumentation in the test consists of pressure cells, vertical force transducers connected to the measuring section, wetted surface measurements using wave gauges tape, accelerometers to determine the accelerations in the rig and the measuring plate, drop velocity measurements, strain measurements using strain gauges in 4 different positions on the plate, vertical deflection of the plate using displacement transducer and wave staffs. The diameter of each pressure cell was 4 *mm*. The instrumentation includes also amplifiers, data logging, storage unit and software written for these tests. The positions of the different transducers connected to the drop rig are shown in Figure 3.

The present problem is difficult to handle experimentally. This is partly due to the very short time duration of an impact associated with an expected very high pressure and partly due to the requirement of high accuracy of the produced models and the generated waves. Compared to conventional model testing, a much higher sampling frequency of the digital recording of the different measurements is required during these tests. Further, the amplifiers have to satisfy requirements to a large frequency range with lines relationship between the measured and amplified results. Sufficiently low rise time and high resonance frequency of the transducers are required for the different transducers. The sampling frequency for most of the transducers was 100 kHz in the tests. Some additional tests were carried out using a sampling frequency of 500 kHz to ensure

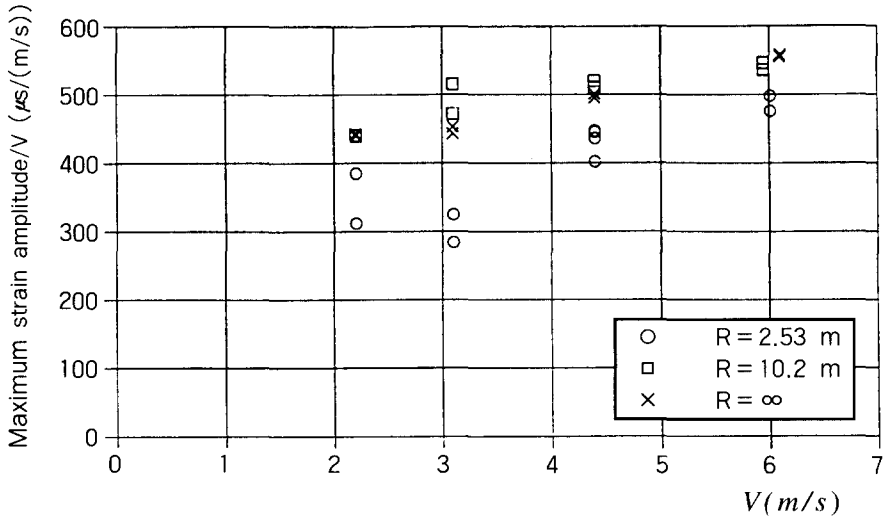

Figure 4. Maximum strain amplitude (in microstrain) in the center of the plate divided by drop speed |V| plotted as a function of the drop speed. R is radius of curvature of the wave crest

that all time series were sufficiently fast recorded.

The tests were carried out for drop speeds ranging from 2.2 *m/s* to 6.2 *m/s* (corresponding to drop heights from 0.25*m* to 2.0*m*). For each drop speed, five different regular wave conditions were used. The radius of curvature of the wave crest R for the different waves varied from 1.5 *m* to 10 *m*. In addition, drop against calm water(i.e. $R = \infty$) was included. The wave crest hits the center of the plate in most cases. This is assumed in the numerical model. However, for some test conditions, the position where the wave crest hits the plate was systematically varied.

The details of the connection between the test plate and the rig are shown in Figure 3. Prior to the drop test, calibration tests were carried out to determine the end connection moment of the plate This moment can be represented as a rotatory spring with spring stiffness K_θ at the plate ends. The end moments were determined from the measured strain distribution in the plate for different point loadings on the plate. The value $k_\theta = 5.7EI/L_B$ was obtained. The drop tests were performed within the linear stress-strain range of the material.

The dry elastic natural frequencies of the plate were determined from free decay tests in air. The natural frequency of the 3 first dry modes are respectively $f_{N1} = 125Hz$, $f_{N2}=375Hz$, $f_{N3} = 800Hz$. The first and third modes are symmetric about the middle of the plate and the second mode is antisymmetric. The structural damping of the first and third modes were respectively 1% and 5% of the critical damping.

4. Analysis and Comparison with Test Data

One of the most important findings from the hydroelastic scaling is that for a given set of structural parameters, the bending stresses in the plate are proportional to the drop speed. By drop speed ve mean the velocity of plate when it initially hits the water. In Figure 4, the maximum strain amplitude measured in the center of the plate divided by the drop speed is shown as a function of the drop speed for the plate. In transforming the measured strains to stresses, 1000 microstrains corresponds to a stress level of 210 N/mm^2. Results for each individual test are

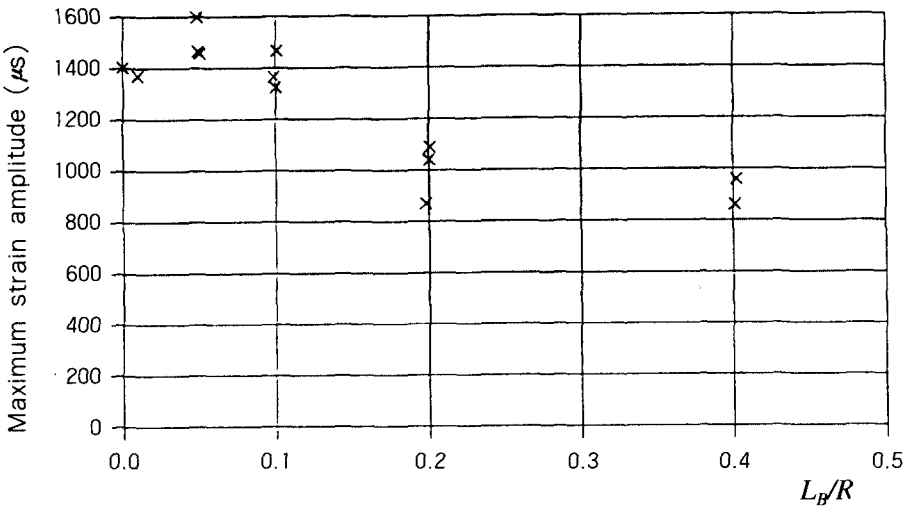

Figure 5. Maximum strain amplitude (in microstrain) in the center of the plate as a function of L_B/R. L_B is the length of the Timoshenko beam and R is radius of curvature of the wave crest. Maximum drop speed is 3.03 *m/s*

shown, so for each test condition, 2-4 test results are presented. The wave crest hits the plate at different locations for the different tests. Except for the tests with the smallest crest radius (R=2.53 *m*), it is seen that the maximum strains are approximately proportional to the drop speed. For not too small R, there is very little scatter between the different individual test results. When R=2.53 *m*, the strains do not follow the above drop speed dependency for the lower drop speeds. For these cases the product of the drop speed and the radius of curvature of the waves is too small in order for the presented scaling to bt the proper scaling of the hydroelastic response, (see the scaling discussion above). Similar dependency of the drop speed was also obtained for the maximum deflection amplitude in the center of the plate and for the maximum hydrodynamic force. Again the radius of curvature was not important as long as it was not too small.

To further investigate the effect of the wave crest radius R on the hydroelastic response, the measured maximum strain amplitudes are plotted as a function of L_B/R in Figure 5. The drop height is $0.5m$ corresponding to a drop speed equal to 3.1 *m/s*. The strains are measured in the center of the plate. Only test results where the wave crest hits within the plate are included. $L_B/R = 0$ represents drop tests against calm water($R = \infty$). The figure shows that the strains are very little affected by the L_B/R ratio when $L_B/R < 0.1$. For higher L_B/R ratios, the strains are found to decrease with decreasing R. For a practical, full scale situation, $L_B/R \approx 1.0m$. Further, wetdeck slamming is mainly a problem for wave lengths λ, corresponding to the natural period of the pitch motions which occurs for $\lambda = 1 \sim 1.5$ times the ship length. Assuming a ship length $L = 80m$ and a wave height of $H = 5m$, gives typically $L_B/R = 0.005 \sim 0.02$. For these values of L_B/R, Figure 5 shows that the strains in the wetdeck are not influenced by the curvature of the waves. Even if the tests are based on regular waves, we anticipate this to be true for irregular waves. But this needs to be tested.

The influence on the strains of where the waves initially hit the wetdeck was investigated by

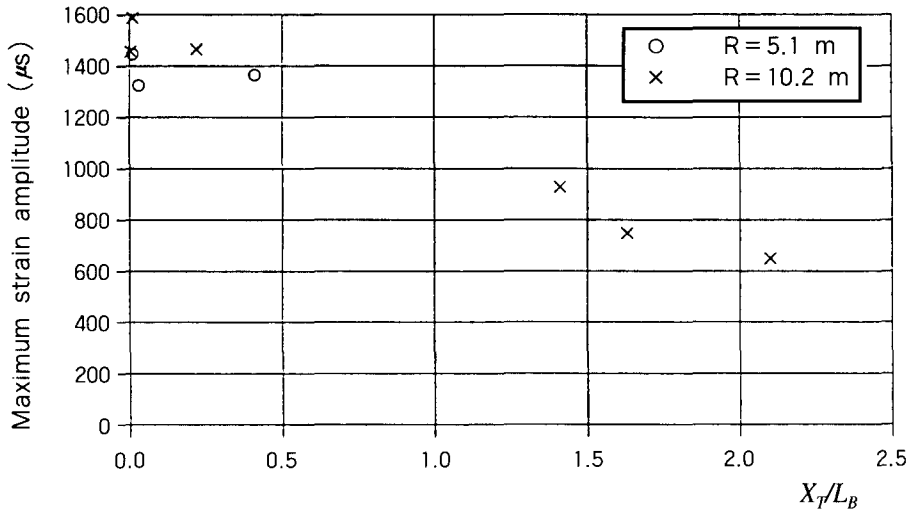

Figure 6. Maximum strain amplitude (in microstrain) in the center of plate as a function of X_T/L_B. L_B is the length of the Timoshenko beam and X_T is the distance between the initial impact position and the center of the plate at the initial impact. Maximum drop speed is 3.03 *m/s*

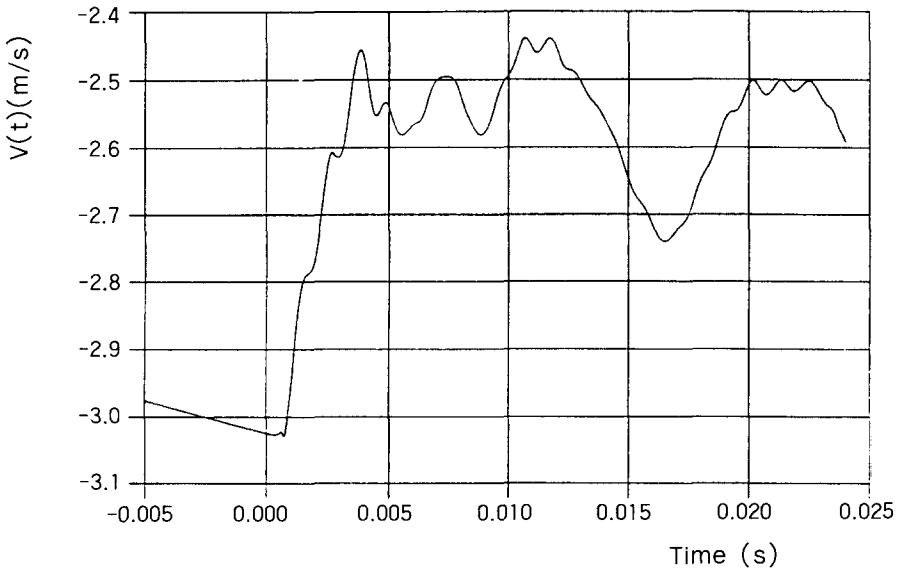

Figure 7. The rigid body velocity of the plate as a function of time. The drop height is 0.5*m*

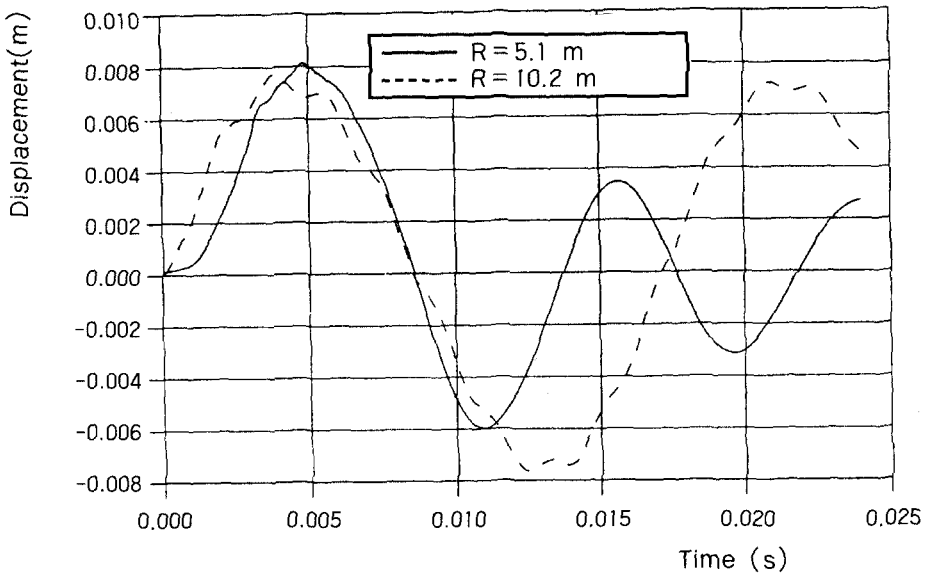

Figure 8. The vertical deflection in the middle of the elastic plate as a function of the time after the initial impact. Results from both the numerical method and the drop tests are reproduced. The drop height is $0.5m$

varying the distance X_T between the center of the plate and the initial wave impact position. The measured strain amplitude in the center of the plate is shown in Figure 6 as a function of X_T / L_B. The results are shown for a drop height of 0.5 m and wave crest radius equal to 5.1 m and 10.2 m. When $X_T / L_B < 0.5$, the strains are approximately independent of the position where the wave crest hits the plate. This agrees with Kvålsvold and Faltinsen [1995].

The numerical solution procedure will now be addressed. A local hydroelastic slamming analysis is carried out. This means we are considering an elastic beam that is forced through the crest of a regular wave system with the same vertical velocity as was measured during the drop tests. 20 dry natural modes are used in the numerical model to approximate the beam deflections. 1% of critical damping is used for all modes. The initial phase of the impact(the compressibility phase) is treated in a simplistic way by using a one-dimensional acoustic approximation. Our results for maximum stresses are not sensitive to this approximation. The radius of curvature of the waves is 10.2 m in the comparative studies between theory and experiments. The rigid body drop velocity of the plate $V(t)$ as a function of time is shown in Figure 7. Three-dimensional flow effects cause a difference in the added mass between the numerical formulation and the model tests. Separate numerical calculations for a rigid flat plate show that the result for the two-dimensional added mass should be reduced by 14%. This reduction implies that the first wet natural period is 6% lower than predicted by a two-dimensional hydrodynamic theory. Since deflections and strains are approximately proportional to the natural period, this implies 6% lower deflection and stress values due to three-dimensional hydrodynamic effects.

Figure 8 shows experimental and numerical values for the vertical deflection midways between the beam ends as a function of the time. Initially, the beam deflection is equal to zero and increases to its maximum value after 4 milliseconds. The oscillation period from the numerical method is approximately 17 milliseconds. This is believed to be close to the lowest wet natural period of the beam since the deflection pattern in time and space is dominated by the first wet

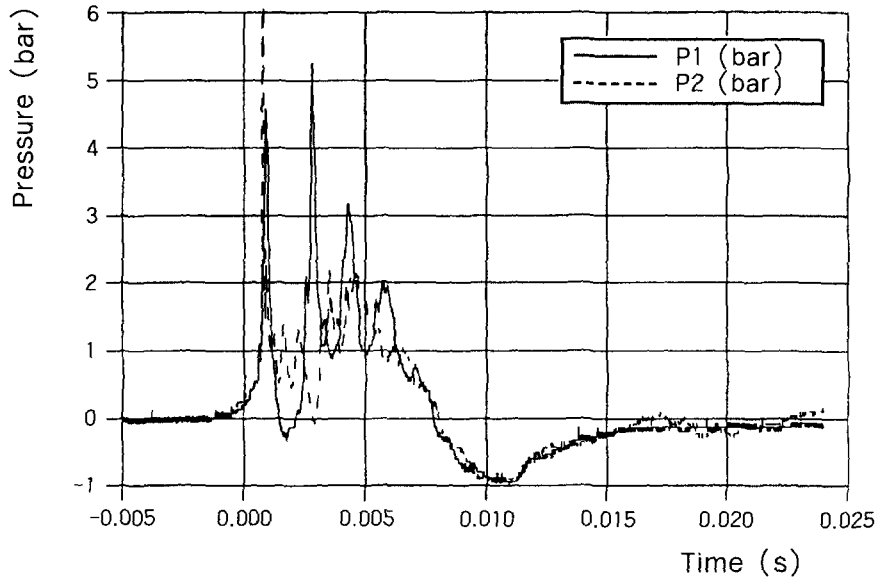

Figure 9. Measured time history of the pressure at two positions of the plate. P1 represents the pressure at the center of the plate and P3 at the position 100 *mm* from the center(see also Figure 3). Drop height is 0.5 *m*

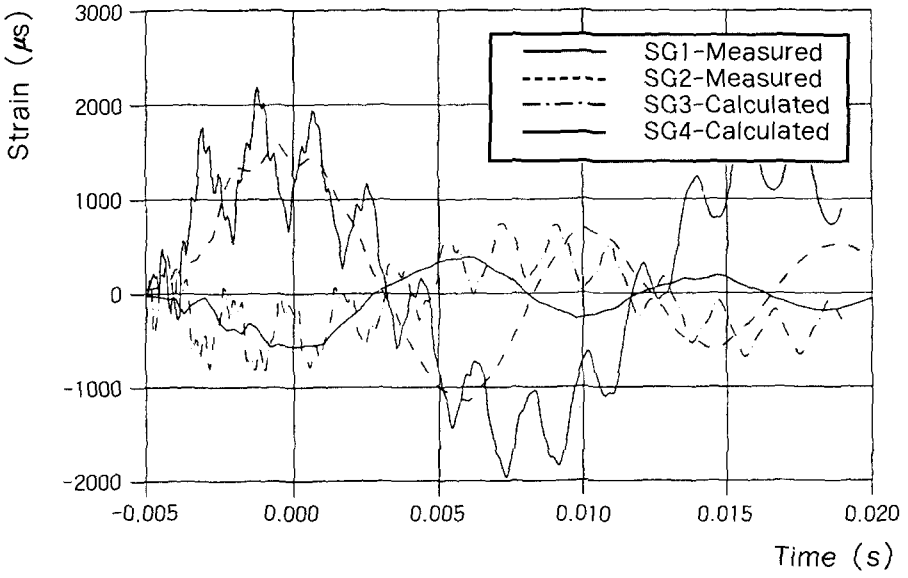

Figure 10. The strains at different locations along the beam and as a function of the time. For details about the strain measurement locations, see Figure 3. The numerical results are compared with the drop test. Drop height is 0.5 *m*

vibration mode. There is good agreement between the experimental and numerical values for the maximum deflection and the oscillation period during the first half oscillation period. However, there is a significant reduction in the experimental values for the maximum deflection and the oscillation period during the second half oscillation period. Since the oscillation period is reduced, this effect cannot be explained by damping. The difference can be explained by the occurrence of cavitation and ventilation in the tests. Figure 9 shows the time history of the measured pressure at two positions at the plate. P1 and P3 represent the pressure in the center of the plate and at a position 100 *mm* from the center (see also Figure 3).

Large underpressures are present in the second half of the oscillation period. The pressures at P1 and P3 are close to the vapor pressure around time equal to 0.01 s. This means cavitation. Due to the large underpressures under the plate during the second half of the first complete oscillation, air will be drawn in under the plate and the pressure becomes close to atmospheric (see time larger than 0.015 s in Figure 9). This means ventilation. This effect is also evident in the measurements of the wetted length, which shows a significant reduction during this time interval. The consequence of this reduction in the effective wetted length due to ventilation and cavitation is a pronounced reduction in the added mass and hence a reduction in the oscillation period. Actually, the oscillation period for time larger than about 0.014 s comes very close to the highest natural period in air. These effects are not included in the numerical model. From a practical design point of view, the maximum deflection and stresses which occurs during the first half oscillation period, are the most important results. For this part of the impact, the numerical and experimental values are in good agreement.

Figure 10 shows the strains at different locations along the beam as a function of time. The strain measurement locations are shown in Figure 3. The numerical method predicts a high frequency oscillation of the strains superposed on the strain oscillation corresponding to the first wet natural period. These oscillations are mainly due to the second symmetric wet mode. These high frequency oscillations are less present in the drop test results. The experimental results corresponding to the second symmetric mode indicate a damping which is about 10% of critical damping. Maximum 5% of this can be explained from the structural tests in air. The theory clearly overpredicts the maximum amplitude of the second symmetric mode. The reason for this must be associated with improper flow description during the initial phases of the impact. An air cushion is for instance likely to be created. However, we have not investigated the cause in any detail. Anyway the amplitude corresponding to the first symmetric wet mode is dominating. The agreement between the numerical calculations and the drop tests is good for the strain contribution from the first wet vibration mode for the different measurement points along the plate during the first half oscillation period. Similarly as for the deflection, the magnitude of the response and the oscillation period are reduced during the second half period of oscillation.

5. Discussion and Application of the Results

Most studies of slamming report only results for the peak pressure. For cases where the local angles between the undisturbed water surface and the wetdeck are small, one knows theoretically and experimentally that the peak pressure is highly time and space dependent. This makes the peak pressure very difficult to detect experimentally, since the results of the peak pressure are sensitive to the exact wave profile and where the waves initially hit the wetdeck relatively to the position of the pressure cells. Additionally, the ratio between the wave crest radius and the diameter of the pressure gauges in the experimental investigations will influence the results of the measured peak pressure. It is also important that the sampling frequency in the measurements is

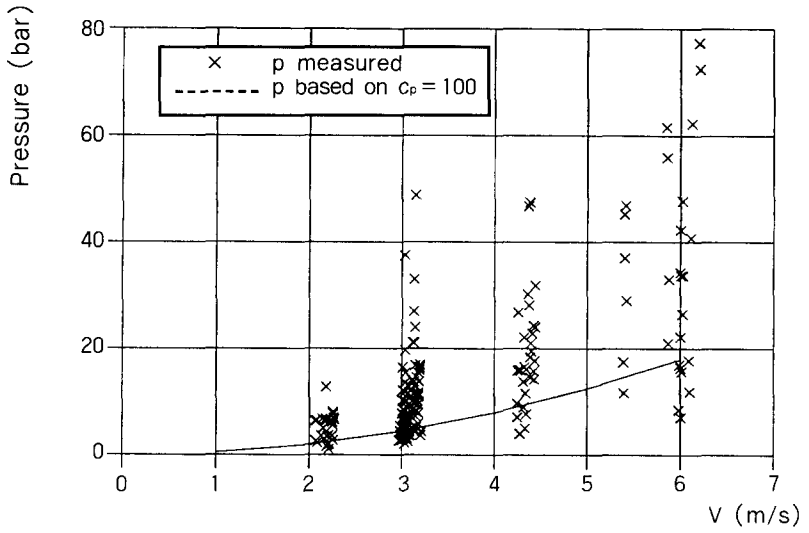

Figure 11. Measured maximum pressure from the different tests as a function of the drop speed. $Cp = p/(1/2\rho|V|^2)$ is the pressure coefficient

sufficiently high to pick up the maximum peak value in time. In Figure 11 the measured peak pressures from all the different drop tests are shown as a function of the drop speed. Clearly, the drop speed is not the only important parameter for the presented results. The results of the peak pressure in Figure 11 are similar to what can be seen in many other experimental slamming investigations. Our theoretical studies show that the peak pressure does not tell anything about maximum bending stresses. The reason is that the high impact pressures last too short and is too concentrated in space to cause any significant force impulse to the local structure. Actually our theory predicts infinite pressure at the edges of the wetted length when the wetted length increases with time. Since our theory is in good agreement with measured strains, it tells that the maximum pressures are not directly influencing the bending stresses. Using the peak pressure as a uniformly distributed pressure in a static analysis will obviously lead to unrealistic local dimensions of the wetdeck. The results of the measured peak pressure in Figure 11 seem chaotic and do not encourage the designer to treat the impact problem in a deterministic way even in deterministic environmental conditions. Our study indicates that wetdeck slamming may ve treated deterministically in deterministic environmental conditions as long as no attention is paid to the peak pressure.

In this study, the wetdeck slamming analysis is treated totally different from earlier analysis we are aware of. What is most important in the analyzed problem is the hydrodynamic load between two transverse stiffeners as a function of time and the dynamic nature of the response in terms of the elastic deformations of the wetdeck What is learned from this study is that the maximum stresses are not sensitive to where the waves initially hit the wetdeck or the radius of curvature of the waves as long as the initial impact speed normal to the wetdeck is not too small. For an ultimate strength analysis, this requirement is easily achieved. This study indicates that under such conditions the maximum bending stresses σ at a fixed position can be written as :

$$\sigma = K_\sigma z_{na} |V| \sqrt{\rho L_B E / I} \tag{1}$$

where K_σ is a function of the longitudinal position between two transverse stiffeners and the beam end boundary conditions. For instance if we apply this relationship to our test case, K_σ is equal to 0.50, 0.33 and 0.15 for X/L_B = 0.0, 0.2 and 0.4, respectively. K_σ is then based on the experimental results in Figure 10. In our test case, z_{nu} is equal to 0.5 h and I is evaluate as $1/12h^3$ where h is the test plate thickness. In the above stress relation, the only parameter that is not dependent on the local geometry, is the impact speed $|V|$. $|V|$ is mainly caused by the global rigid ship motions, which are Froude scaled. If the simple stress relation is sufficient to express the hydroelastic response of the wetdeck, it is very easy to use the stress relation in a statistical model to establish realistic values of the bending stresses to be used directly in the design of the wetdeck. However, there are effects that need to be further studied before any final conclusions of the hydroelastic response can be made. For instance, this formulation needs to be generalized so that the wetdeck is not modelled locally as one beam. A formulation where the wetdeck is modelled as three beams were studied by Kvålsvold and Faltinsen [1995]. They accounted for the asymmetry of the local fluid flow. They concluded also that the stresses in the wetdeck were not sensitive to where waves hit the wetdeck. Their conclusion is supported by the present drop test results, see Figure 6. However, more validation tests with models and full scale ships in realistic wave conditions are needed.

The interaction effects between the local fluid flow and the global rigid ship motions have been investigated by Kvålsvold and Faltinsen [1993]. Their study only covers the two first impact phases, but they concluded that the interaction effects had a minor effect on the impact loads. It is believed that their conclusion is valid for the third impact phase as well, since the third impact phase is mainly a decay oscillation of the beam with the initial conditions determined from the second impact phase.

Conclusions

The local hydroelastic response due to slamming against the wetdeck of a multihull vessel in a head sea wave system is investigated numerically and experimentally. Hydroelastic effects are found to be very important. The theoretical hydrodynamic load model is a generalization of Wagner's two-dimensional asymptotic theory [Wagner 1932]. A beam model is used to model a longitudinal stiffener between two transverse stiffeners. This study shows how to scale the local hydroelastic response of the wetdeck. The impact is then separated into three different impact phases. The three impact phases are called the compressibility phase, the structural inertia phase and the added mass-restoring phase. There is a time scale associated with each impact phase. The third time scale, where the maximum stresses in the wetdeck occur, is associated with the lowest wet natural period of the beam. Agreement between the numerical method and the drop tests is reported. For not too small impact speeds $|V|$, a simple relation is found between the maximum local stress in the wetdeck, the wetdeck geometry, the properties of the wetdeck material and the initial impact velocity. It is found that the maximum stress is not sensitive to where the waves hit the wetdeck and the curvature of the wave crests in the impact region. For smaller impact speeds, the maximum stresses in the wetdeck are dependent of the radius of curvature of the wave crest. It is stated that measurements of peak pressures during wetdeck slamming do not tell anything about maximum stresses. This study suggests that one should measure strains and relative rigid body velocities between the vessel and the waves in the impact region. This conclusion should not be generalized to other slamming cases where the largest impact pressures are not highly concentrated in space and time.

References

[1] Aarsnes, J.V., 1994, An experimental investigation of the effect of structural elasticity on slamming loads and structural response, Technical report, MARINTEK A/S.

[2] Kvålsvold, J. and Faltinsen, O.M., 1993, Hydroelastic modelling of slamming against the wetdeck of a catamaran, Proc. 2nd Int. Conf. on Fast Sea Transportation, FAST'93. Yokohama, Japan, Vol 1, pp. 681-697, Published by the Society of Naval Architects of Japan.

[3] Kvålsvold, J. and Faltinsen, O.M. ,1994, Slamming loads on wetdecks of multihull vessels, Proc. Int. Conf. Hydroelasticity in Marine Technology, Trondheim, Norway, pp. 205-220, Published by A.A. Balkema, Rotterdam.

[4] Kvålsvold, J. and Faltinsen, O.M. ,1995, Hydroelastic modelling of wetdeck slamming on multihull vessels, To be published in J. Ship Research.

[5] Meyerhoff, W.K. ,1965, Die Berechnung hydroelastischer Stosse, Schiffstech, Vol. 12,60.

[6] Wagner, H. ,1932, Uber Stoss und Gleitvergange an der Oberflache von Flussigkeiten, Zeitschr. f. Angewendte Mathematik und Mechanic, Vol. 12, pp. 192-235.